

## Supplementary Information

High-loading Fe<sub>1</sub> sites on vanadium disulfides: a scalable and non-defect-stabilized single atom catalyst for electrochemical nitrogen reduction

*Yunxia Liu,<sup>a</sup> Xing Fan,<sup>a</sup> Wenyi Bian,<sup>a</sup> Yingke Yang,<sup>a</sup> Peipei Huang,<sup>b</sup> Werner A Hofer,<sup>c</sup> Hui Huang,<sup>a\*</sup> Haiping Lin,<sup>b\*</sup> Youyong Li,<sup>a,d\*</sup> and Shuit-Tong Lee<sup>a,d</sup>*

<sup>a</sup>Institute of Functional Nano & Soft Materials (FUNSOM), Jiangsu Key Laboratory for Carbon-Based Functional Materials and Devices, Soochow University, Suzhou 215123, China.

<sup>b</sup>School of Physics and Information Technology, Shaanxi Normal University, Xi'an 710119, China.

<sup>c</sup>University of Chinese Academy of Sciences, Chinese Academy of Sciences, P.O. Box 603, Beijing 100190, China.

<sup>d</sup>Macao Institute of Materials Science and Engineering, Macau University of Science and Technology, Taipa 999078, Macau SAR, China

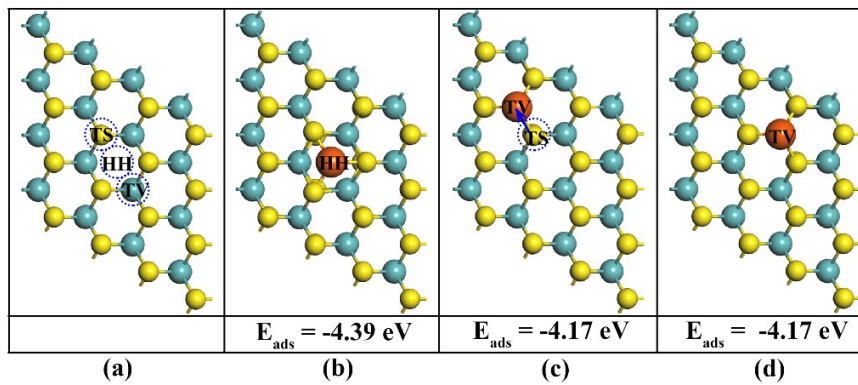
\*Corresponding authors: [hhuang0618@suda.edu.cn](mailto:hhuang0618@suda.edu.cn), [hplin@snnu.edu.cn](mailto:hplin@snnu.edu.cn), and [yyli@suda.edu.cn](mailto:yyli@suda.edu.cn)

## 1. Fe adsorption on a VS<sub>2</sub> monolayer.

There are three possible high symmetry adsorption sites for Fe atoms on a VS<sub>2</sub> monolayer, namely the TV, TS, and HH sites (on-top site of a V atom, on-top of a S atom and at the three-fold hollow site). In our simulations we considered a  $4 \times 4$  supercell of VS<sub>2</sub> monolayer to minimize interactions between Fe atoms in the periodic supercell. The adsorption configurations of single Fe atom on these possible adsorption sites as well as the relevant adsorption energies are shown in Fig. S1. The adsorption energies ( $E_{ads}$ ) of single Fe atoms on the VS<sub>2</sub> monolayer were calculated with the equation:

$$E_{ads} = E_{adsorbed} - E_{VS_2} - E_{Fe} \quad (S1)$$

We find that the HH site is energetically the most favorable.



**Fig. S1** (a) The on-top site of S, on-top site of V, and the hollow site is referred to as “TS”, “TV” and “HH”, respectively. (b-c) shows adsorption structures and corresponding adsorption energies of the Fe atom on these sites. The Fe atom initially at the “TS” site moved to the “TV” site upon structural relaxation. The yellow, green and orange balls represent S, V and Fe atoms, respectively.

## 2. Thermal stability of Fe<sub>1</sub>/VS<sub>2</sub>.

First-principles molecular dynamics calculations have been performed to investigate the thermal stability of the Fe<sub>1</sub>/VS<sub>2</sub> catalysts. Figure S2 shows the root-mean-square deviation of the single Fe atom on a VS<sub>2</sub> monolayer at 300 K and 400 K. The RMSD curves with respect to the simulation time show that Fe<sub>1</sub>/VS<sub>2</sub> reaches stable equilibrium after 300 femtoseconds. As the maximum RMSD of Fe<sub>1</sub>/VS<sub>2</sub> at 300 K and 400 K are only 0.145 Å and 0.157 Å, the atomic structures should not change significantly, indicating good thermal stability for temperatures as high as 400K.

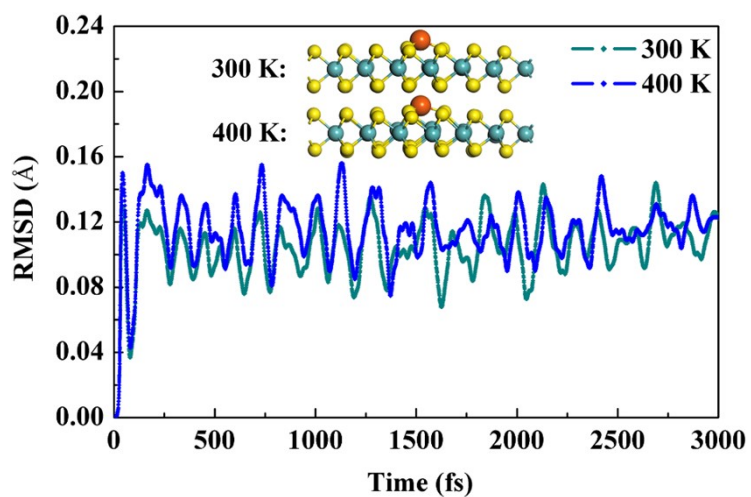


Fig. S2 Molecular dynamics simulation and analysis of the Fe<sub>1</sub>/VS<sub>2</sub> in root-mean-square deviations (RMSD) at 300 K (green) and 400K (blue).

### 3. The diffusion of Fe atom on the VS<sub>2</sub> monolayer.

DFT calculation shows that the diffusion barrier of the Fe atom on a VS<sub>2</sub> surface is about 0.99 eV, indicating a very low probability of clustering of Fe atoms at ambient conditions.

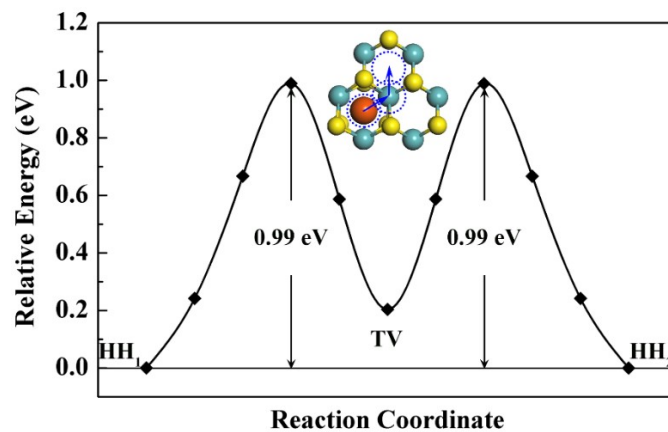
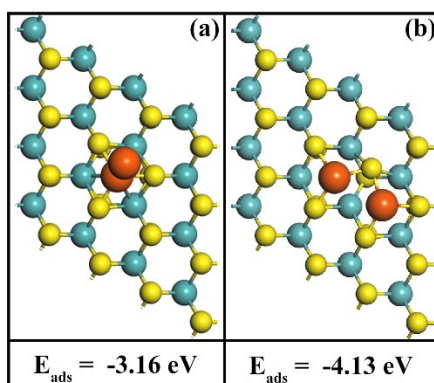


Fig. S3 The energy profile of the Fe diffusion on the VS<sub>2</sub> surface.

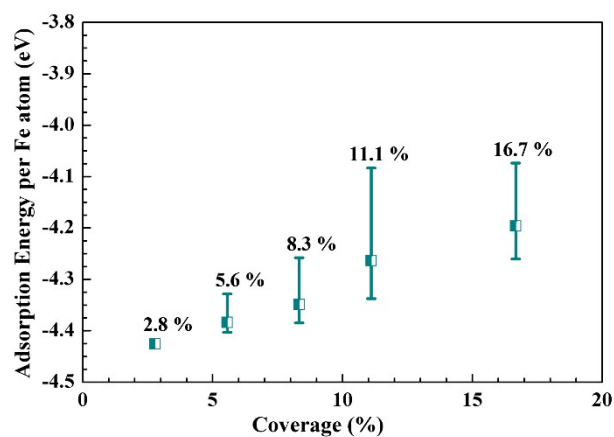
#### 4. Configurations of Fe dimer and two Fe atoms adsorbed on the VS<sub>2</sub> monolayer.



**Fig. S4** Atomic configurations of (a) a Fe dimer and (b) two Fe atoms adsorbed on a VS<sub>2</sub> monolayer. The yellow, green and orange balls represent S, V and Fe atoms, respectively.

The averaged adsorption energy per Fe atom in the Fe dimer is -3.16 eV, which is much higher than that of two adjacent HH site Fe atoms (-4.13 eV, Fig. 1(b)). Such significant increase of energies indicates that the Fe dimer is not likely to form during Fe diffusion.

#### 5. The atomic adsorption energies of Fe at different coverages.



**Fig. S5** The atomic adsorption energy of Fe<sub>1</sub>/VS<sub>2</sub> with respect to Fe coverages. The averaged adsorption energies per Fe atom at different Fe coverages are shown as squares. Error bars are employed to indicate the range of adsorption energies per Fe atom at given Fe coverages.

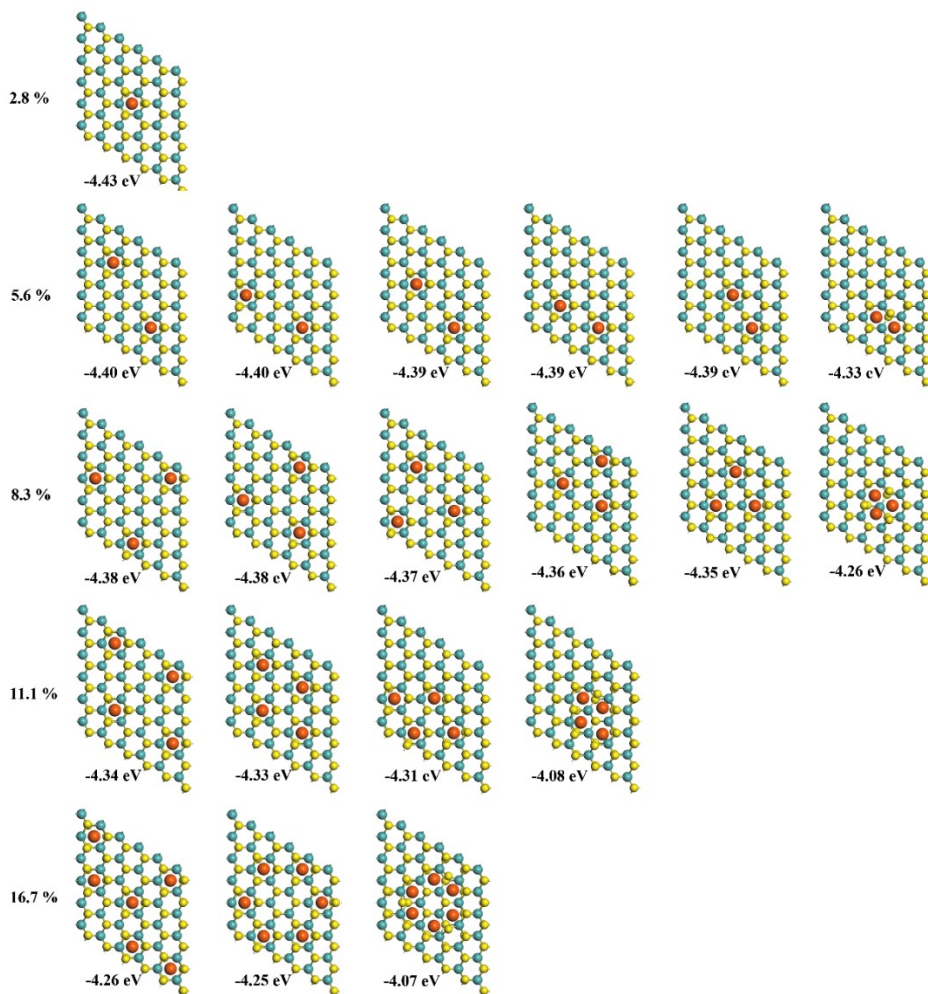
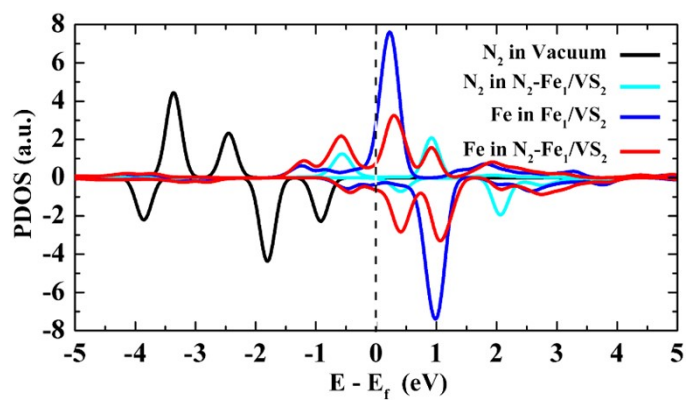



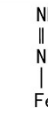


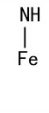
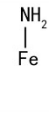
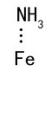

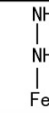
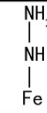
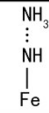
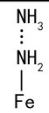

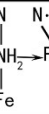
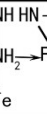
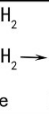
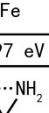

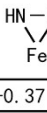
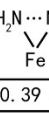
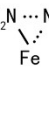
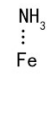

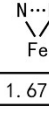
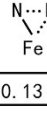
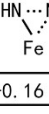
Fig. S6 Configurations and corresponding adsorption energies of different Fe coverages on non-defective VS<sub>2</sub>.

## 6. PDOS plots of N<sub>2</sub> adsorption on the Fe<sub>1</sub>/VS<sub>2</sub>.



**Fig. S7** The PDOS of the N<sub>2</sub> in vacuum (black), N<sub>2</sub> in N<sub>2</sub>-Fe<sub>1</sub>/VS<sub>2</sub> (cyan), Fe in Fe<sub>1</sub>/VS<sub>2</sub> (blue) and Fe in N<sub>2</sub>-Fe<sub>1</sub>/VS<sub>2</sub> (red).

## 7. The evolution of Gibbs free energies along various reaction pathways.

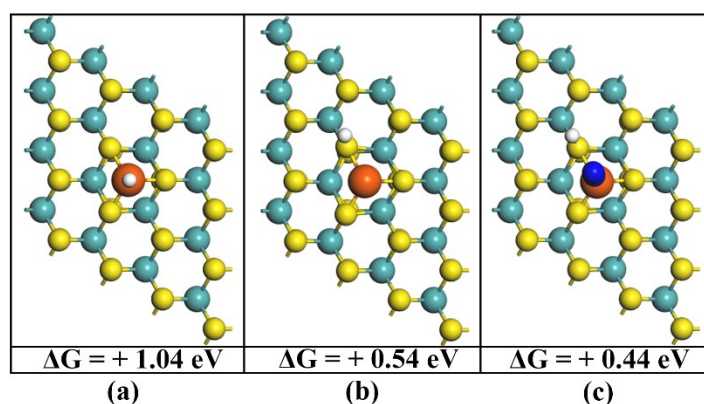
N <sub>2</sub> -end-on	1H	2H	3H	4H	5H	6H
 -0.15 eV						
		0.21 eV	0.90 eV	1.11 eV	-0.12 eV	-2.04 eV
						
	0.54 eV	0.62 eV	-0.67 eV	0.38 eV		
						
0.72 eV	1.67 eV	-0.37 eV	0.38 eV	-1.30 eV		
N <sub>2</sub> -side-on	1H	2H	3H	4H	5H	6H
 0.89 eV						
		0.97 eV	-0.37 eV	-0.39 eV		
						
	0.72 eV	1.67 eV	0.13 eV	-0.16 eV	-2.06 eV	-2.04 eV

**Fig. S8** The structures and changes of Gibbs free-energies of various potential intermediates along the reaction path of NRR on the Fe<sub>1</sub>/VS<sub>2</sub>.

## 8. Competitive HER side reaction.

To perform well as an electrochemical catalyst, the Fe<sub>1</sub>/VS<sub>2</sub> system must be stable in a proton-rich solution which is different from the typical Haber-Bosch process. In the proton-rich solution, the Fe<sub>1</sub>/VS<sub>2</sub> may be poisoned by hydrogen in an acidic solution before N<sub>2</sub> molecules can bind to the catalyst. It is therefore necessary to examine the effect of hydrogen for Fe<sub>1</sub>/VS<sub>2</sub>. Under the electrochemical conditions for an NRR electrons will be injected into Fe<sub>1</sub>/VS<sub>2</sub>; as a result, positively charged protons will be attracted and can combine with electrons to form adsorbed hydrogen. A 4x4 VS<sub>2</sub> supercell was simulated to investigate the effect of proton attachment for NRR. The results indicate that the H atom has only weak interaction with the Fe<sub>1</sub>/VS<sub>2</sub> surface due to positive Gibbs free-energies. A H atom adsorbed on the Fe atom has a Gibbs free energy of +1.04 eV (Fig. S9a) and surrounding the Fe atom of +0.54 eV (Fig. S9b). The results allow the conclusion that the active Fe<sub>1</sub>/VS<sub>2</sub> center will not be rapidly covered by hydrogen under electrochemical condition. This outcome has a similar cause as the strong repulsion between single adsorbed Fe atoms on this surface, the positive charging upon adsorption. Additional simulations of

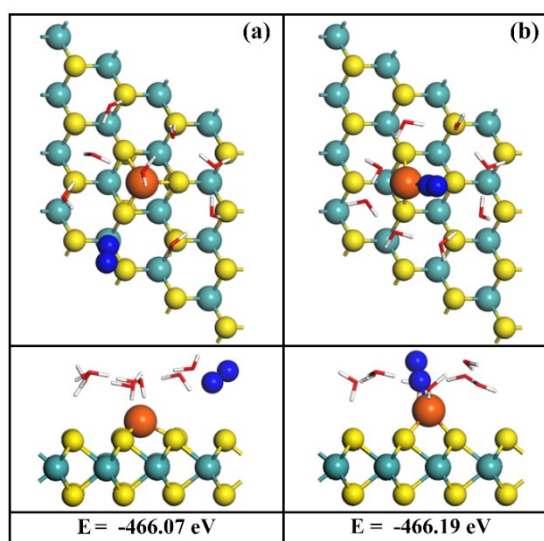
H surrounding the  $\text{N}_2\text{-Fe}_1/\text{VS}_2$ , with a Gibbs free energy of +0.44 eV (Fig. S9c) lead to the same conclusion. Hydrogen poisoning for this catalyst is therefore not a concern. The catalytic inertness of base planes toward HER have also been reported in other  $\text{MS}_2$  materials.<sup>1,2</sup>



**Fig. S9** The change of Gibbs free energy upon H adsorption (a) on the Fe atom of  $\text{Fe}_1/\text{VS}_2$ , (b) on one of the three S atoms that are next to the bare Fe atom, and (c) on one of the three S atoms surrounding the  $\text{N}_2$  adsorbed Fe atom. The change of Gibbs free energy per H adsorption is 1.04 eV, 0.54 eV and 0.44 eV, respectively.

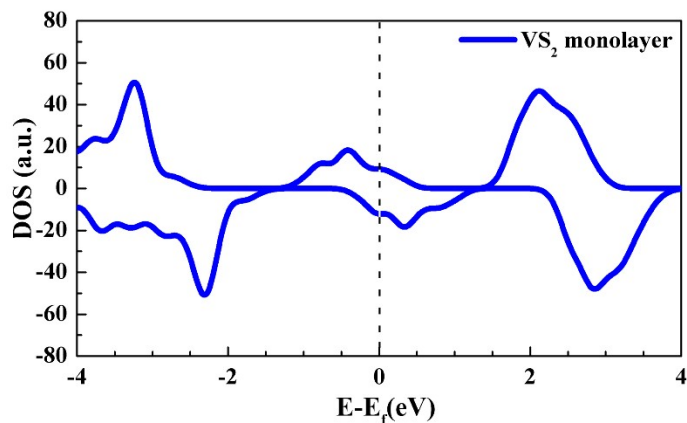
## 9. Solvent effect.

Eight  $\text{H}_2\text{O}$  molecules and a  $\text{N}_2$  molecule were added to a  $4 \times 4$   $\text{Fe}_1/\text{VS}_2$  supercell in order to evaluate the bonding of  $\text{N}_2$  and  $\text{H}_2\text{O}$  on  $\text{Fe}_1/\text{VS}_2$ . In Fig. S10(a), all  $\text{H}_2\text{O}$  molecules are close to the Fe atom while the  $\text{N}_2$  molecule was far away from Fe. Moreover, the  $\text{N}_2$  molecule is moved close to Fe site and be surrounded with  $\text{H}_2\text{O}$  molecules in the Fig. S10(b). As seen in Fig. S10, the total energy decreased by 0.12 eV ( $E_b - E_a$ ) when  $\text{N}_2$  takes the place of an adsorbed  $\text{H}_2\text{O}$ . Therefore, the  $\text{N}_2$  molecule would be preferable than  $\text{H}_2\text{O}$  on  $\text{Fe}_1/\text{VS}_2$ , namely water molecules would not block the catalytic site.



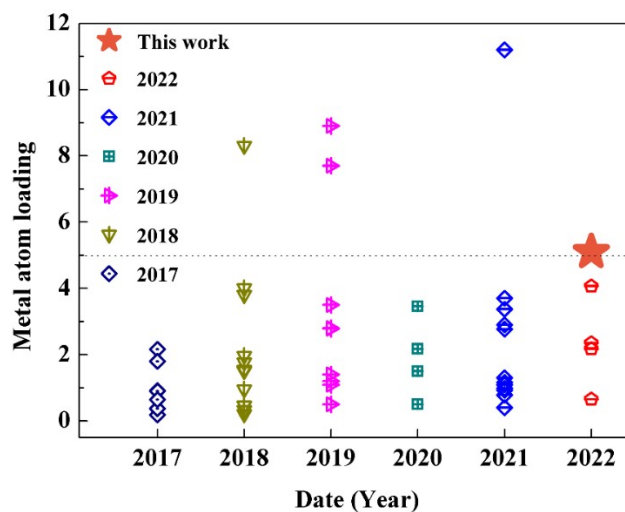
**Fig. S10** Atomic configurations of the Fe single atom site covered with 8 H<sub>2</sub>O and 1 N<sub>2</sub> molecules. (a) All H<sub>2</sub>O molecules are close to the Fe atom while the N<sub>2</sub> molecule was far away from Fe. (b) The N<sub>2</sub> molecule is moved close to Fe.

### 10. The DOS of a VS<sub>2</sub> monolayer.



**Fig. S11** The DOS plot of a VS<sub>2</sub> monolayer.

### 11. The loading of metals in recently reported Fe SACs.



**Fig. S12** Comparison of Fe loading between Fe<sub>1</sub>/VS<sub>2</sub> and recently reported Fe single-atom catalysts.

### 12. Table S1. Comparison of Fe loading between Fe<sub>1</sub>/VS<sub>2</sub> and recently reported Fe single-atom catalyst.

Materials	Loading [ICP]	Ref.
-----------	---------------	------



Fe <sub>1</sub> /VS <sub>2</sub>	5.1 wt% (calculated)	This work
SA Fe-g-C <sub>3</sub> N <sub>4</sub>	4.07 wt%	<i>Chem. Eng. J.</i> , <b>2022</b> , 427,130803
Fe SA/NPCs	2.17 wt%	<i>Small</i> , <b>2022</b> , 18, 2104941
Fe SAC-MOF-5	2.35 wt%	<i>Adv. Energy Mater.</i> , <b>2022</b> , 12, 2102688
Fe-N-C SACs	0.65 wt%	<i>Chem. Eng. J.</i> , <b>2022</b> , 430, 132882
Fe-N-C	1.3 wt%	<i>Angew. Chem. Int. Ed.</i> , <b>2021</b> ,60, 25296 –25301
Meso-Fe-N-C	2.9 wt%	<i>J. Mater. Chem. A</i> , <b>2021</b> ,9, 19489-19507
Fe-SAC/NPC	0.4 wt%	<i>Angew. Chem. Int. Ed.</i> , <b>2021</b> ,60, 23614 –23618
Co <sub>2</sub> /Fe-N@CHC	0.98 wt%	<i>Adv.Mater.</i> , <b>2021</b> , 33, 2104718
Fe/NC	2.9 wt%	<i>Small Methods</i> , <b>2021</b> , 5, 2001165
Bi <sub>4</sub> O <sub>5</sub> I <sub>2</sub> -Fe <sub>30</sub>	1.09 wt%	<i>ACS Materials Lett.</i> , <b>2021</b> , 3, 4, 364–371
Fe <sub>1</sub> /CN	11.2 wt%	<i>Angew. Chem. Int. Ed.</i> , <b>2021</b> ,60, 21751 –21755
SAFe@NG	3.7 wt%	<i>Adv. Mater.</i> <b>2021</b> , 33, 2007090
Fe <sub>SA</sub> -NO-C-900	0.78 wt%	<i>Angew. Chem. Int. Ed.</i> <b>2021</b> , 60, 9078 –9085
HSAC/Fe-4	3.37 wt%	<i>Adv. Sci.</i> 2021, 8, 2002249 □
Fe-N-C	0.93 wt%	<i>J. Energy Chem.</i> <b>2021</b> , 54, 579–586
Fe-C/Al <sub>2</sub> O <sub>3</sub>	1.16 wt%	<i>Sep. Purif. Technol.</i> <b>2021</b> , 54, 258118086
Fe <sub>1</sub> /N-DG	2.77 wt%	<i>J. Hazard. Mater.</i> <b>2021</b> , 412, 125162
Fe <sub>SA</sub> -N-C	3.46 wt%	<i>Nat. Commun.</i> <b>2020</b> , 11, 2831.
Fe <sub>1</sub> /C-PPh <sub>3</sub> /NaI	0.5 wt%	<i>ACS Catal.</i> <b>2020</b> , 10, 5502-5510.
Fe SA/NPCs	2.17 wt%	<i>Appl. Catal. B</i> <b>2020</b> , 278, 119270.
Fe-NC SAC	1.5 wt%	<i>J. Mater. Chem. A</i> <b>2020</b> , 8, 9981.
FeN <sub>5</sub> SA/CNF	1.2 wt%	<i>Sci. Adv.</i> <b>2019</b> , 5, eaav5490.
Fe <sup>3+</sup> -N-C	2.8 wt%	<i>Science</i> <b>2019</b> , 364, 1091–1094.
TPI@Z8(SiO <sub>2</sub> )-650-C	2.78 wt%	<i>Nat. Catal.</i> <b>2019</b> , 2, 259.
Fe <sub>SA</sub> -N-C	1.09 wt%	<i>Nat. Commun.</i> <b>2019</b> , 10, 341.
Fe-N-C HNSs	1.4 wt%	<i>Adv. Mater.</i> <b>2019</b> , 31, 1806312.
FeSA-G	7.7 wt%	<i>Adv. Sci.</i> <b>2019</b> , 6, 1802066.
Fe-N/C-CNTs	0.50 wt%	<i>ACS Catal.</i> <b>2019</b> , 9, 336.
Fe SAs/N-C	3.5 wt%	<i>ACS Catal.</i> <b>2019</b> , 9, 2158-2163.
Fe-NC SAC	8.9 wt%	<i>Nat. Commun.</i> <b>2019</b> , 10, 1278.
Fe-NHGF	0.2 wt%	<i>Nat. Catal.</i> <b>2018</b> , 1, 63.
Fe-SAs/NPS-HC	1.54 wt%	<i>Nat. Commun.</i> <b>2018</b> , 9, 5422.
Fe SAs-N/C-20	0.20 wt%	<i>J. Am. Chem. Soc.</i> <b>2018</b> , 140, 11594.
FeN <sub>4</sub> /GN	4.0 wt%	<i>Chem</i> <b>2018</b> , 4, 1902.
Fe-N <sub>4</sub> SAs/NPC	1.96 wt%	<i>Angew. Chem. Int. Ed.</i> <b>2018</b> , 57, 8614.
FeSA-N-C	1.76 wt%	<i>Angew. Chem. Int. Ed.</i> <b>2018</b> , 57, 8525.

Fe-ISA/SNC	0.95 wt%	<i>Adv. Mater.</i> <b>2018</b> , <i>30</i> , 1800588.
NDC-900	0.46 wt%	<i>Adv. Energy Mater.</i> <b>2018</b> , <i>8</i> , 1701771.
FeSAs/PTF	8.3 wt%	<i>ACS Energy Lett.</i> <b>2018</b> , <i>3</i> , 883.
FeCl1N4/CNS	1.5 wt%	<i>Energy Environ. Sci.</i> <b>2018</b> , <i>11</i> , 2348.
Fe-N-C-950	0.32 wt%	<i>ACS Catal.</i> <b>2018</b> , <i>8</i> , 2824.
Fe-N/C-1/30	3.8 wt%	<i>Nano Energy</i> <b>2018</b> , <i>52</i> , 29-37.
Fe-N-C	0.91 wt%	<i>Small</i> <b>2018</b> , <i>14</i> , 1704282.
ISA Fe/CN	2.16 wt%	<i>Angew. Chem. Int. Ed.</i> <b>2017</b> , <i>56</i> , 6937.
NDC-900	0.18 wt%	<i>Adv. Energy Mater.</i> <b>2017</b> , <i>8</i> , 1701771.
Fe-N-C-600	1.8 wt%	<i>J. Am. Chem. Soc.</i> <b>2017</b> , <i>139</i> , 10790.
SA-Fe/CN.	0.9 wt%	<i>J. Am. Chem. Soc.</i> <b>2017</b> , <i>139</i> , 10976.
Fe©N-C-12	0.37 wt%	<i>ACS Catal.</i> <b>2017</b> , <i>7</i> , 7638.
C-AFC©ZIF-8	0.64 wt%	<i>Nano Energy</i> <b>2017</b> , <i>38</i> , 281.
FePhenMOF-ArNH <sub>3</sub>	0.5 wt%	<i>Energy Environ. Sci.</i> <b>2016</b> , <i>9</i> , 2418.

**13. Table S2. Magnetic moments of Fe during the NRR process.**

Distal pathway	$\mu_B$ (Fe) ( $\mu_B$ )	Alternating pathway	$\mu_B$ (Fe) ( $\mu_B$ )
00-N <sub>2</sub> -end-on	2.799	00-N <sub>2</sub> -end-on	2.799
01-N-NH	1.566	01-N-NH	1.566
02-N-NH <sub>2</sub>	2.155	02-NH-NH	2.833
03-N-NH <sub>3</sub>	0.812	03-NH-NH <sub>2</sub>	2.726
04-NH	1.698	04-NH-NH <sub>3</sub>	1.854
05-NH <sub>2</sub>	3.083	05-NH <sub>2</sub> -NH <sub>3</sub>	2.750
06-NH <sub>3</sub>	0.008	06-NH <sub>3</sub>	0.008

Enzymatic pathway	$\mu_B$ (Fe) ( $\mu_B$ )	Hybrid pathway	$\mu_B$ (Fe) ( $\mu_B$ )
00-N <sub>2</sub> -side-on	2.226	00-N <sub>2</sub> -end-on	2.799
01-NH-N	2.319	01-N-NH	1.566
02-NH-NH	-0.305	02-N-NH <sub>2</sub>	2.155
03-NH <sub>2</sub> -NH	2.334	03-NH-NH <sub>2</sub>	2.726
04-NH <sub>2</sub> -NH <sub>2</sub>	2.446	04-NH <sub>2</sub> -NH <sub>2</sub>	2.446
05-NH <sub>3</sub> -NH <sub>2</sub>	2.241	05-NH <sub>3</sub> -NH <sub>2</sub>	2.241
06-NH <sub>3</sub>	0.008	06-NH <sub>3</sub>	0.008

## References

1. J. Xu, G. Shao, X. Tang, F. Lv, H. Xiang, C. Jing, S. Liu, S. Dai, Y. Li, J. Luo and Z. Zhou, *Nat. Commun.*, **2022**, *13*, 2193.
2. J. Zhang, C. Zhang, Z. Wang, J. Zhu, Z. Wen, X. Zhao, X. Zhang, J. Xu and Z. Lu, *Small*, **2018**, *14*, 1703098.

